In conclusion, we found for the first time a positive relationship between a long sleep duration and some markers of melanoma aggressiveness. Future studies are needed to investigate the main pathophysiological mechanisms that could explain this association and the prognostic relevance of this finding.

Funding

The authors have nothing to declare in relation to this manuscript.

Conflict of interest

The authors declare that they have no conflict of interest.

Bibliografía

1. Kakizaki M, Kuriyama S, Sone T, Ohmori-Matsuda K, Hozawa A, Nakaya N, et al. Sleep duration and the risk of breast cancer: the Ohsaki Cohort Study. Br J Cancer. 2008;99:1502–5.
2. Zhang X, Giovannucci EL, Wu K, Gao X, Hu F, Ogino S, et al. Associations of self-reported sleep duration and snoring with colorectal cancer risk in men and women. Sleep. 2013;36:681–8.
3. Martinez-Garcia MA, Campos-Rodriguez F, Nagore E, Martorell A, Rodriguez-Peralto JL, Riveiro-Falkenbach E, et al. Sleep-disordered breathing is independently associated with increased aggressiveness of cutaneous melanoma: a multicenter observational study in 443 patients. Chest. 2018;154:1348–58.
4. -Gershenwald JE, Scolyer RA, Hess KR, Sondak VK, Long GV, Ross MI, et al. Melanoma staging: evidence-based changes in the American Joint Committee on Cancer Eighth edition cancer staging manual. CA Cancer J Clin. 2017;67:472–92.
5. Born J, Lange T, Hansen K, Molle M, Fehm HL. Effects of sleep and circadian rhythm on human circulating immune cells. J Immunol. 1997;158:4454–64.
6. Irwin MR, Olmstead R, Carroll JE. Sleep disturbance, sleep duration, and inflammation: a systematic review and meta-analysis of cohort studies and experimental sleep deprivation. Biol Psychiatry. 2016;80:40–52.
7. Patel SR, Zhu X, Storfer-Isser A, Mehra R, Jenny NS, Tracy R, et al. Sleep duration and biomarkers of inflammation. Sleep. 2009;32:200–4.
8. Lauderdale DS, Knutson KL, Yan LL, Liu K, Rathouz PJ. Sleep duration: how well do self-reported reflect objective measures? The CARDIA Sleep Study. Epidemiology. 2008;19:838–45.

Jose Daniel Gómez Olivas [a], Francisco Campos-Rodriguez [b], Eduardo Nagore [c], Luis Hernández [d], Valentin Cabriada [e], Jorge Abad [f], Olga Mediano [g], Esther Pastor [h], Eusebi Chiner [h], Manuel Sanchez de la Torre [i], Irene Cano [j], Maria Somoza [k], Alberto Garcia-Ortega [a], Grace Oscullo [a], Miguel Angel Martinez-García [a,*]

[a] *Pneumology Department. Hospital Universitario y Politecnico La Fe, Valencia, Spain*
[b] *Pneumology Department Hospital Valme.IBiS, Sevilla, Spain*
[c] *Oncology Department, Instituto Valenciano de Oncología, Spain*
[d] *Pneumology Department Hospital General Alicante, Spain*
[e] *Pneumology Department Hospital Cruces, Bilbao, Spain*
[f] *Sleep Unit, Hospital Germans Trials i Pujol, Barcelona, Spain*
[g] *Pneumology Department Hospital de Guadalajara, Spain*
[h] *Pneumology Department Hospital San Juan Alicante, Spain*
[i] *Research Department, Hospital A. Vilanova, Lleida, Spain*
[j] *Pneumology Department, Hospital Getafe, Madrid, Spain*
[k] *Pneumology Department, Consorcio Sanitario Terrassa, Barcelona, Spain*

* Corresponding author.
E-mail address: mianmartinezgarcia@gmail.com (M.A. Martinez-García).

https://doi.org/10.1016/j.arbres.2020.10.020

Comparing Probe-Based Confocal Laser Endomicroscopy With Histology. Are We Looking at the Same Picture?

Comparando endomicroscopía confocal con histología. ¿Estamos mirando la misma imagen?

Dear Editor,

Probe-based confocal laser endomicroscopy (pCLE) provides real-time vision of respiratory tissues at the cellular level through a flexible bronchoscope. This technique might guide sampling of pulmonary nodules,[1–4] lymph nodes[5] or pleural biopsies.[6] First studies of the respiratory tract were performed with a 488 nm wavelength probe that allows elastin visualization without adding fluorophores in the tissue. Because cells are not visualized, lung cancer pattern descriptions were limited to changes on the stromal component.[1,7–9] Later studies used fluorophores like methylene blue or fluorescein that could be excited at a 488 or a 660 nm wavelength, respectively, to visualize cell nuclei.[2,4,10] In these studies, different imaging patterns were described. In particular, healthy tissue was described as having homogeneous architecture with bright, partially overlapping nuclei. Inflammation was considered when heterogeneous tissue architecture without overlapping nuclei but expanded cytoplasms were observed, and neoplasia was reported as a chaotic distribution of dark cells with heterogeneous nuclei.[2,8,9,11,12] Although pictures of these patterns were frequently presented together with pictures of histology samples, none of the studies correlated the measurements performed in pCLE images to those of histology samples. In this pilot study, we aimed to explore

Table 1
Measurements Performed in the Histological Samples (Optical Microscopy) and pCLE Images.

	Final Diagnosis	Optical Microscopy (H&E Stain, 40× Magnification)	Probe-based Confocal Laser Endomicrosocopy	*P*-Value
Number of nuclei	Normal ($n=6$)	28.8 (5.78)	35.3 (4.13)	.1025
Mean (SD)	Pathological ($n=9$)	33.8 (16.2)	27.8 (16.6)	.8946
Mean size of nuclei (μm^2)	Normal ($n=6$)	103 [90.8;129]	36.5 [31.7;40.9]	<.05
Median [Q1;Q3]	Pathological ($n=9$)	127 [114;155]	29.5 [27.9;59.0]	<.05
Relative area occupied by nuclei (μm^2)	Normal ($n=6$)	60.6 (18.2)	26.5 (10.8)	<.05
Mean (SD)	Pathological ($n=9$)	80.1 (13.4)	38.9 (14.3)	<.05

Pathological refers to inflammation or malignancy.
H&E: haematoxylin–eosin, SD: standard deviation.

the feasibility of correlating pCLE and optical microscopy features of normal and pathological airway samples.

Under general anesthesia and orotracheal intubation with a rigid bronchoscope (Efer-Dumon type, La Ciotat, France) pCLE was performed after applying a drop of 1% MB in nine regions of normal mucosa and in six tumors, as determined with white-light bronchoscopy. The AlveoFlex® probe and a laser scanning unit equipped with 660 nm laser wavelength (Cellvizio®, Mauna Kea Technologies, Paris, France) were used. After pCLE image registration, biopsies were taken and histology was studied with optical microscopy following haematoxylin-eosin (H&E) staining. A total of 15 patients were studied. The biopsies revealed normal epithelium in 6 cases, inflammatory infiltrate in 3 cases and thoracic tumors in 6 cases, which included B cell lymphoma, adenocarcinoma, squamous cell carcinoma, small cell lung cancer, and non-small cell lung cancer. The study was approved by the local ethics review board (Clinical Research Ethics Committee of Bellvitge University Hospital – Act 08/13) and written informed consent was obtained from all participants.

One representative image from the pCLE registration was selected and compared to one image of the H&E-stained sample. Nuclei were segmented in all images using ImageJ software (National Institutes of Health, Bethesda, MD, USA).[13] In the pCLE images, we accounted for the number and mean size of nuclei, the relative area occupied by nuclei and the intensity of fluorescence. In the H&E-stained histological sample images, we accounted for the number and mean size of nuclei and the relative area occupied by nuclei. We chose these features because these structures can be identified both in the optical and the pCLE images.

We made two different comparisons. First, we compared the patterns of pCLE alone. A logistic regression model was fitted to predict the probability of pathological tissue (inflammation or malignancy) based on every feature. We observed that changes in these features were associated with variations in the probability of disease. In particular, we observed that the odds of disease increased by a factor of 1.03 (95% CI: 0.99–1.07) for every one unit increase in the mean size of nuclei, by a factor of 1 (95% CI: 1–1) for every one unit increase in the intensity of fluorescence, and by a factor of 1.088 (95% CI: 1.01–1.224) for every one unit increase in the relative area occupied by nuclei. Next, we registered the measurements performed in the optical microscopy and pCLE images (see Table 1) and compared their distributions. After a Wilcoxon rank sum exact test we observed that the distributions of the mean size and relative area occupied by nuclei were different in the images of optical compared to pCLE microscopy. Although this small analysis is not adequately powered to achieve statistical significance, our results of the pCLE alone patterns are in line with the previously mentioned studies showing that it is possible to discern between normal and pathological tissue patterns, while the measurements performed in the optical microscopy and pCLE images cannot be correlated to the tissue structures observed in the biopsy specimens.

Our pilot study supports the use of pCLE to identify patterns of normal and pathological airway tissue but discourages comparisons between pCLE and histology images. These findings might reflect that the final histology diagnosis is based on a set of information not obtainable from a sequence of nuclei as it is observed in pCLE images. To empower pCLE as a useful tool for diagnosis of lung cancer, future studies should focus on identifying further discriminative features[14] or specific tumor markers. Otherwise, this technique will be limited to the identification of pathological areas for biopsy guidance.

Authors' Contributions

M.D-F, B.T. and A.R. generated the hypothesis; M.D-F., B.T. and N.B. designed the study; M.D-F., B.T, N.B, N.C, R.L., J.D and A.R contributed to data acquisition. C.T. performed the statistical analysis, and M.D-F. wrote the manuscript. All members of the study critically reviewed the submitted article for important intellectual content, provided final approval of the version to be published, and agreed to be accountable for all aspects of the work and to ensure that any questions related to the accuracy or integrity of any part of the work will be appropriately investigated and resolved.

Funding

This work was supported by grants from Fundació La Marató de TV3, SEPAR 2018, FUCAP-Albert Agustí and SOCAP.

Conflict of Interest

All authors of this manuscript report that no potential conflicts of interest exist with any companies/organizations whose products or services may be discussed in this article.

Bibliografía

1. Wellikoff AS, Holladay RC, Downie GH, Chaudoir CS, Brandi L, Turbat-Herrera EA. Comparison of in vivo probe-based confocal laser endomicroscopy with histopathology in lung cancer: a move toward optical biopsy. Respirology. 2015;20:967–74.
2. Hassan T, Piton N, Lachkar S, Salaun M, Thiberville L. A novel method for in vivo imaging of solitary lung nodules using navigational bronchoscopy and confocal laser microendoscopy. Lung. 2015;193:773–8.
3. Hassan T, Thiberville L, Hermant C, Lachkar S, Piton N, Guisier F, et al. Assessing the feasibility of confocal laser endomicroscopy in solitary pulmonary nodules for different part of the lungs, using either 0.6 or 1.4 mm probes. PLOS ONE. 2017;12:e0189846.
4. Thiberville L, Salaun M, Lachkar S, Dominique S, Moreno-Swirc S, Vever-Bizet C, et al. Confocal fluorescence endomicroscopy of the human airways. Proc Am Thorac Soc. 2009;6:444–9.
5. Wijmans L, de Bruin DM, Meijer SL, Annema JT. Real-time optical biopsy of lung cancer. Am J Respir Crit Care Med. 2016;194:e10–1.
6. Wijmans L, Baas P, Sieburgh TE, de Bruin DM, Ghuijs PM, van de Vijver MJ, et al. Confocal laser endomicroscopy as a guidance tool for pleural biopsies in malignant pleural mesothelioma. Chest. 2019;156:754–63.
7. Filner JJ, Bonura EJ, Lau ST, Abounasr KK, Naidich D, Morice RC, et al. Bronchoscopic fibered confocal fluorescence microscopy image characteristics and pathologic correlations. J Bronchol Intervent Pulmonol. 2011;18:23–30.
8. Sorokina A, Danilevskaya O, Averyanov A, Zabozlaev F, Sazonov D, Yarmus L, et al. Comparative study of ex vivo probe-based confocal laser endomicroscopy and light microscopy in lung cancer diagnostics. Respirology. 2014;19:907–13.
9. Shah PL, Kemp SV, Newton RC, Elson DS, Nicholson AG, Yang GZ. Clinical correlation between real-time endocytoscopy, confocal endomicroscopy, and histopathology in the central airways. Respiration. 2017;93:51–7.
10. Fuchs FS, Zirlik S, Hildner K, Schubert J, Vieth M, Neurath MF. Confocal laser endomicroscopy for diagnosing lung cancer in vivo. Eur Respir J. 2013;41:1401–8.
11. Fuchs FS, Zirlik S, Hildner K, Frieser M, Ganslmayer M, Schwarz S, et al. Fluorescein-aided confocal laser endomicroscopy of the lung. Respiration. 2011;81:32–8.
12. Wellikoff AS, Holladay RC, Downie GH, Chaudoir CS, Brandi L, Turbat-Herrera EA. Comparison of in vivo probe-based confocal laser endomicroscopy with histopathology in lung cancer: a move toward optical biopsy. Respirology. 2015;20:967–74.
13. Schindelin J, Arganda-Carreras I, Frise E, Kaynig V, Longair M, Pietzsch T, et al. Fiji: an open-source platform for biological-image analysis. Nat Meth. 2012;9:676–82.
14. Rakotomamonjy A, Petitjean C, Salaün M, Thiberville L. Scattering features for lung cancer detection in fibered confocal fluorescence microscopy images. Artif Intell Med. 2014;61:105–18.

Marta Diez-Ferrer[a,*], Benjamin Torrejon-Escribano[b], Nuria Baixeras[c], Cristian Tebe[d,e], Noelia Cubero[a], Rosa Lopez-Lisbona[a], Jordi Dorca[a], Antoni Rosell[f]

[a] Department of Respiratory Medicine, Hospital de Bellvitge-IDIBELL-University of Barcelona, Barcelona, Spain
[b] Unit of Advanced Optical Microscopy, Scientific and Technological Centers (CCiTUB) University of Barcelona, L'Hospitalet de Llobregat, Barcelona, Spain
[c] Department of Pathology, Hospital de Bellvitge-IDIBELL-University of Barcelona, Barcelona, Spain
[d] Biostatistics Unit, Bellvitge Biomedical Research Institute (IDIBELL). L'Hospitalet de Llobregat, Barcelona, Spain
[e] Department of Basic Medical Sciences, Universitat Rovira i Virgili, Reus, Tarragona, Spain
[f] Thorax Institute, Hospital Germans Trias i Pujol-IGTP-UAB, Badalona, Barcelona, Spain

[*] Corresponding author.
E-mail address: marta.diez@bellvitgehospital.cat (M. Diez-Ferrer).

https://doi.org/10.1016/j.arbres.2021.01.020

Mediastinitis ascendente necrosante. Un caso excepcional

Ascending Necrotizing Mediastinitis. An Exceptional Case

Estimado Director:

La mediastinitis necrosante (MN) se define como la progresión de una infección aguda a distancia hacia el mediastino[1] con el compromiso de sus componentes[2,3], asociado a la necrosis de los tejidos involucrados. Se trata de una complicación poco frecuente pero potencialmente letal, con una mortalidad que oscila del 10 al 40% según las series[4], una alta morbilidad derivada de la gravedad del proceso[4] y la necesidad de ingreso prolongado en la mayoría de los casos[2].

El foco más frecuentemente asociado son las infecciones del área otorrinolaringológica[1], generalmente a partir de un absceso odontógeno u orofaríngeo[5], y menos frecuentemente a partir de infecciones cervicales[4,6]. La propagación de la infección se produce a través de la fascia profunda retrofaríngea[6], pretraqueal o vascular[7], facilitada por la presión negativa intratorácica, la gravedad y la respiración[1,4,7]. Esto ha llevado a la denominación clásica de MN descendente. La propagación a través de un origen distinto a la cabeza y el cuello es excepcional, aunque otros focos como abdominales, de pared torácica, pulmonares, de nódulos linfáticos e incluso por diseminación hematógena[1] han sido descritos.

Presentamos a un paciente de 83 años con antecedentes de hipertensión y diabetes mellitus tipo 2, fibrilación auricular permanente anticoagulada, bloqueo auriculoventricular completo con implante de marcapasos y síndrome de apnea obstructiva del

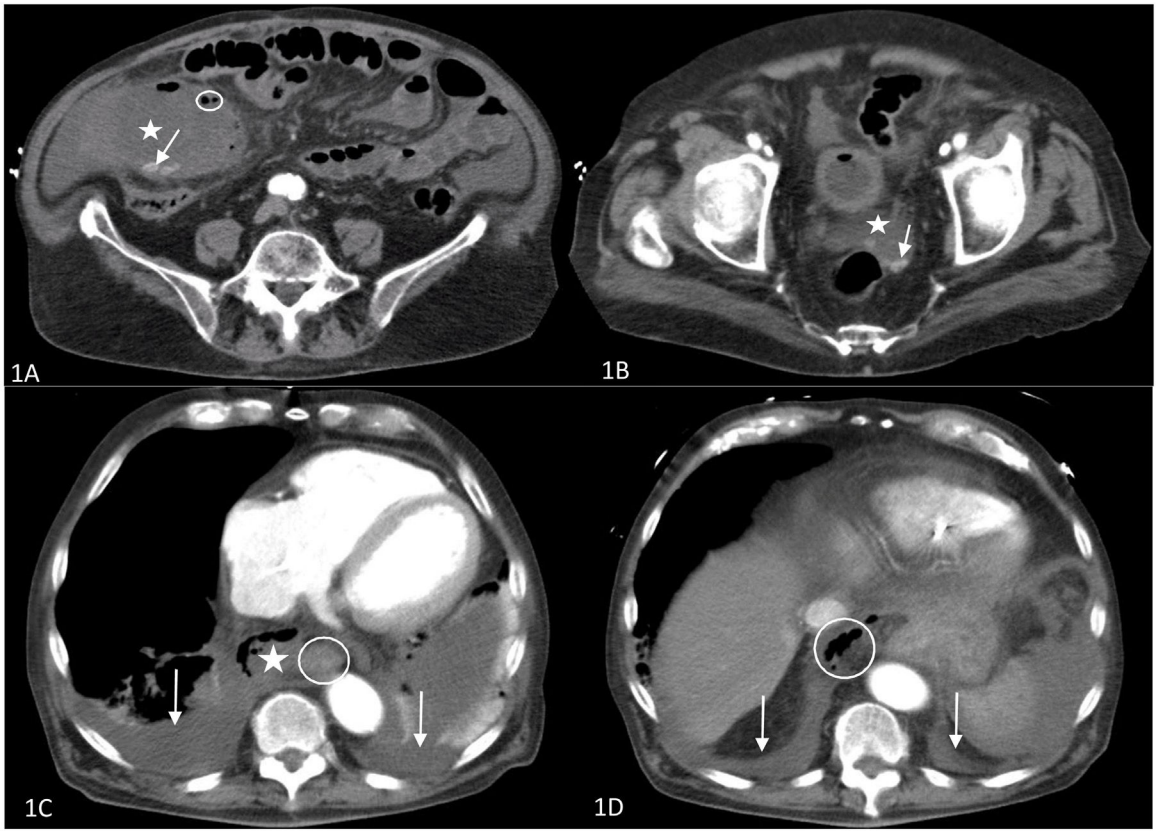

Figura 1. A y B: TAC abdominal. 1A: Vesícula biliar (asterisco) aumentada de tamaño, con litiasis en su interior (flecha) y gas libre en la pared de la vesícula (rodeado) indicativo de colecistitis enfisematosa. 1B: Fondo de saco de Douglas con líquido libre en su interior (asterisco), así como litiasis (flecha), que evidencian bilioperitoneo. C y D: TAC torácica. 1C: Cortes torácicos altos; colección mediastínica con aire en su interior (asterisco); esófago (rodeado); derrame pleural bilateral (flechas). 1D: Cortes toracoabdominales; cúpulas diafragmáticas (flecha); aire retroperitoneal (rodeado) en progresión al tórax.